

# Attenuation Induced by Water Vapor along Earth-Space Links: Selecting the Most Appropriate Prediction Method

L. Luini, C. Riva, and L. Emiliani

**Abstract**—This communication presents an improved approximate method for the estimation of water vapor attenuation along Earth-space slant paths, over the 1-350 GHz frequency range. Evaluated against a large set of radiosonde data, the proposed method provides more accurate results than those delivered by the current alternative approximation methods included in Annex 2 of recommendation ITU-R P.676-10. This result is important as it sheds light on which approximate water vapor attenuation model should be selected for predictions along Earth-space slant paths.

**Index Terms**— Attenuation, atmospheric modeling, millimeter wave propagation, satellite communication

## I. INTRODUCTION

Attenuation induced by water vapor in the troposphere,  $A_v$ , contributes to total attenuation along a satellite link. Although its magnitude is in the orders of a few tenths of dBs in the Ku band, it becomes appreciable for Ka and Q/V band links (~1 to 2 dB) [1], and will impact the clear sky spectral efficiency achievable by the satellite communication service.

Various techniques exist to quantify  $A_v$ : from complex ones making use of full vertical profiles of the troposphere (pressure  $P$ , temperature  $T$  and relative humidity  $RH$ ) [2],[3], to approximations receiving as input the surface water vapor density  $\rho_s$  or the integrated water vapor content  $V$  [4]. For example, the ITU-R includes in recommendation P.676-10 [5] the three approaches mentioned above and, in addition, provides in recommendation P.836-5 the necessary reference data for  $\rho_s$  and  $V$  to be used as input to the simplified methodologies when local data are not available [6]. Given the availability of different prediction methods within recommendation 676-10, it is worth assessing their prediction accuracy in order to provide guidance in selecting the most appropriate methodology.

This paper builds upon the work in [7], which presents an improvement to the ITU-R P.676-10 simplified method receiving as input  $V$ . Specifically, the enhancement consists in extending its application range from 20-100 GHz to 1-350 GHz (the full frequency interval addressed in recommendation ITU-R P.676-10). In addition, we address the question of which among the available approximations should be used for the analysis of satellite links. To support our recommendation, we will test the prediction performance of each model against  $A_v$

values obtained by the MPM93 mass absorption model [2] using as input an extensive set of radiosonde observation (RAOBS) data (vertical profiles of  $P$ ,  $RH$  and  $T$ ; 10 years of measurements over 24 sites worldwide).

The remainder of the paper is structured as follows: Section II provides details on the RAOBS dataset; Section III reviews the simplified prediction methods included in recommendation ITU-R P.676-10 and introduces the improved model. Section IV presents the results of the testing activity and, finally, Section V draws some conclusions.

## II. THE RADIOSONDE DATABASE

Radiosonde observations (RAOBS) are key to electromagnetic wave propagation modeling, as they provide high-resolution information on the state of the atmosphere, from which the impact of water vapor and oxygen on millimeter waves can be accurately estimated [2],[3],[8]. In this contribution, we take advantage of a highly reliable 10-year set of RAOBS data covering the whole Globe.

The FERAS radiosounding dataset was assembled by the FUB (Fondazione Ugo Bordonni) under an ESA (European Space Agency) funded activity, starting from a National Center for Atmospheric Research (NCAR) database. It consists of vertical profiles of pressure  $P$ , temperature  $T$  and relative humidity  $RH$ , collected over 24 sites, twice a day (0 and 12 Coordinated Universal Time – UTC) for ten years (1980-1989) in non-rainy conditions.

Fig. 1 illustrates the locations part of the FERAS set, covering different climates, e.g. from cold in Finland, to Mediterranean in Italy or to equatorial in Singapore.



Fig. 1. Sites where RAOBS data were collected.

A detailed description of the FERAS database can be found in the final report of the COST 255 project [9], which also lists the principles according to which all RAOBS data were checked and validated. Besides taking into account original NCAR quality control marks, plausibility and inconsistency checks were applied. For example: the validity range of ground pressure was set to 700-1100 hPa, RAOBS levels corresponding to inversions of pressure or height values were discarded, and the validity range of temperature and dew point temperature was set to 183-333 K for the whole profile. Finally, after this pre-processing, outliers of the time series of integrated parameters such as the total water vapor content were identified and removed.

Manuscript received xxx.

Lorenzo Luini and Carlo Riva are with the Dipartimento di Elettronica, Informazione e Bioingegneria, Politecnico di Milano, Milano, Italy, and with the Istituto di Elettronica e di Ingegneria dell'Informazione e delle Telecomunicazioni (IEIIT), CNR, Milano, Italy (e-mail: lorenzo.luini@polimi.it).

L. Emiliani is with SES S.A., Luxembourg. (e-mail: ldemiliani@ieee.org).

### III. METHODS FOR SLANT PATH WATER VAPOR ATTENUATION PREDICTION

Recommendation ITU-R P.676-10 provides, in Annexes 1 and 2, three different methodologies for the prediction of water vapor absorption with different levels of accuracy [5].

Annex 1 contains the most refined and accurate method to predict path attenuation due to water vapor,  $A_V$ , based on the knowledge of full vertical profiles of  $P$ ,  $T$  and  $RH$ . Given the complexity of such an approach, which sits upon the MPM93 mass absorption model proposed by Liebe in [2], Annex 2 proposes two approximated methodologies, both of which rely on less demanding input parameters. Details on these approximations, as well as of an improvement introduced in [7], are provided in the following subsections.

#### A. Method A: the ITU-R Approach Based on Surface Water Vapor Content ( $\rho_S$ )

The first approximation to calculate  $A_V$  is based on the surface specific attenuation due to water vapor,  $\gamma_w$ , obtained from the surface pressure  $P_S$ , temperature  $T_S$  and water vapor content  $\rho_S$  ( $\text{g}/\text{m}^3$ ). Specifically,  $\gamma_w$  is calculated using an analytical expression derived from curve-fitting the results provided by the more accurate method included in Annex 1. An additional component of this method is the equivalent water vapor height  $h_w$ , which depends on  $P_S$  as well, and is derived under the assumption of a standard exponential trend of the water vapor content  $\rho$  with height  $h$  [5]:

$$\rho(h) = \rho_S \exp(h/V_{SH}) \quad (1)$$

In (1),  $V_{SH}$ , typically referred to as water vapor scale height, regulates the decay rate of  $\rho$ .

As a result, the path attenuation due to water vapor at frequency  $f$  is obtained as:

$$A_V^A = \frac{\gamma_w(f, P_S, \rho_S, T_S) h_w(P_S)}{\sin \theta} \quad (2)$$

Equation (2) indicates that the zenithal path attenuation (the numerator) is scaled to the slant path with elevation angle  $\theta$  (valid only for  $\theta \geq 5^\circ$ ) using the cosecant approach, which, in turn, assumes that the spatial variability of water vapor is fairly limited. As noted in [5], a limitation in the prediction accuracy of this method might come from  $h_w$ : the water vapor scale height  $V_{SH}$  typically exhibits variability with latitude, season and climate, all of which are not reflected in  $h_w$ , as it only depends on the ground pressure.

The reader is addressed to [5] for more details on the prediction method including a comprehensive description of its mathematical expressions.

#### B. Method B: the ITU-R Approach Based on Integrated Water Vapor Content ( $V$ )

The second approximate method included in Annex 2 of [5] receives as input the integrated water vapor content  $V$  in mm. Specifically, for a zenithal path (slant paths are addressed using

the cosecant scaling approach as for Method A):

$$A_V^B(f) = a_V(f_{ref}) \frac{\gamma_w(f, P_{ref}, \rho_{ref})}{\gamma_w(f_{ref}, P_{ref}, \rho_{ref})} V = \tilde{a}_V(f, V) V \quad (3)$$

with:

$$\begin{aligned} P_{ref} &= 780 \text{ hPa} \\ \rho_{ref} &= V/V_{SH,ref} \text{ g}/\text{m}^3 \\ V_{SH,ref} &= 4 \text{ km} \end{aligned}$$

Method B relies on the fact that the ratio between the specific water vapor attenuation  $\gamma_w$  at a reference frequency  $f_{ref} = 20.6$  GHz and at the target frequency  $f$  is approximately equal to the ratio of the path attenuation  $A_V(f_{ref})/A_V(f)$ , as well as on the mass absorption coefficient  $a_V(f_{ref}) = 0.0173$ , which turns out to be almost independent of the site [10].

Finally, though  $\gamma_w$  in (2) and (3) are the same, in the latter, the dependence of  $\gamma_w$  on temperature has been omitted as it is linked to  $\rho_{ref}$  through:

$$T_{ref} = 14 \ln(0.22 \rho_{ref}) + 3 \text{ } ^\circ\text{C} \quad (4)$$

The reader is directed to [9] for a complete description of the method.

#### C. Method C: Refinement of the ITU-R Approach Based on Integrated Water Vapor Content ( $V$ )

Reference [7] improves the accuracy of Method B by introducing the dependence of the mass absorption coefficient  $\tilde{a}_V(f, V)$  on the site altitude  $h_0$ . Specifically, equation (3) is extended to:

$$A_V^C = a_V(f_{ref}) \frac{\gamma_w(f, P_{ref}, \rho_{ref})}{\gamma_w(f_{ref}, P_{ref}, \rho_{ref})} (a h_0^b + 1) V = \tilde{a}_V(f, V, h_0) V \quad (5)$$

where  $h_0$  ( $< 4$  km) is expressed in km. Coefficients  $a$  and  $b$  in (5) were determined using as reference the RAOBS dataset described in Section II, with half the reference sites used for deriving the coefficients, and the other half for model testing. Specifically, the regression of  $a$  and  $b$  was achieved by comparing the Complementary Cumulative Distribution Function (CCDF) of  $A_V$ , coupling RAOBS-derived vertical profiles of  $P$ ,  $T$  and  $RH$  with the MPM93 mass absorption model, with the same statistics derived from (5) [8]. The input values of  $V$  were taken from RAOBS data.

In this contribution, an improvement to [7], consisting in the extension of the applicability range, from 20-100 GHz range to the full 1-350 GHz interval currently addressed in recommendation ITU-R P.676-10, is presented. The regression exercise was repeated using the same FERAS sites of [7]. As a result,  $a$  and  $b$  have the following expression:

$$a = 0.2048 \exp \left[ - \left( \frac{f - 22.43}{3.097} \right)^2 \right] + 0.2326 \exp \left[ - \left( \frac{f - 183.5}{4.096} \right)^2 \right] + 0.2073 \exp \left[ - \left( \frac{f - 325}{3.651} \right)^2 \right] - 0.1113 \quad (6)$$

$$b = 8.741 \cdot 10^4 \exp(-0.587f) + 312.2f^{-2.38} + 0.723 \quad (7)$$

Furthermore, the reference pressure  $P_{ref}$  and water vapor scale height  $V_{SH,ref}$  are set to:

$$P_{ref} = 815 \text{ hPa and } V_{SH,ref} = 3.67 \text{ km} \quad (8)$$

Finally,  $a_V(f_{ref})$  is updated to 0.0176, such that the final expression to calculate  $A_V$  becomes:

$$A_V^C = \begin{cases} 0.0176 \frac{\gamma_w(f, P_{ref}, \rho_{ref})}{\gamma_w(f_{ref}, P_{ref}, \rho_{ref})} (ah_0^b + 1) V & 20 < f \leq 350 \text{ GHz} \\ 0.0176 \frac{\gamma_w(f, P_{ref}, \rho_{ref})}{\gamma_w(f_{ref}, P_{ref}, \rho_{ref})} V & 1 \leq f < 20 \text{ GHz} \end{cases} \quad (9)$$

#### IV. MODELS' REVIEW: PREDICTION ACCURACY

We proceed in this Section to assess the performance of each of the models outlined in section III, by comparing their predictions against the CCDF delivered by the MPM93 mass absorption model coupled with the FERAS dataset introduced in Section II. For each prediction method, the necessary inputs were extracted from ITU-R recommendation P.836-5 [6].

The prediction error is calculated in terms of average (E) and Root Mean Square (RMS) of the following metric, derived from recommendation ITU-R P.311-15 [11]:

$$\varepsilon(P) = \begin{cases} 100 \left( \frac{A_V(P)}{10} \right)^{0.2} \ln \left( \frac{A_V^*(P)}{A_V(P)} \right) & A_V(P) < 10 \text{ dB} \\ 100 \ln \left( \frac{A_V^*(P)}{A_V(P)} \right) & A_V(P) \geq 10 \text{ dB} \end{cases} \quad (10)$$

$A_V^*(P)$  and  $A_V(P)$  in (10) are the water vapor attenuation values extracted from the estimated and RAOBS-derived attenuation statistics, respectively, relative to the same probability level  $P \geq 0.05\%$ .

Fig. 2 shows a sample comparison between the reference RAOBS-derived statistics of  $A_V$  and those estimated using the three methods. Specifically, RAOBS refers to Stornway (UK) and the frequency is  $f = 80$  GHz. Fig. 2 indicates that, in this case, Method C and Method A offer the best and worst prediction performance, respectively. Fig. 3 and Fig. 4 offer a

better overview of the methods' prediction performance, confirming the observation of Fig 2. The figure legend reports the overall mean E ( $\psi_E$ ) and mean RMS ( $\psi_{RMS}$ ) associated to each prediction method.

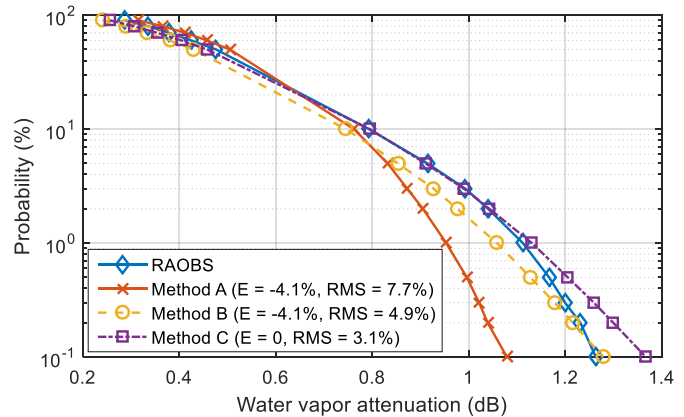


Fig. 2. Zenithal water vapor attenuation CCDF at 80 GHz calculated according to RAOBS data + MPM93 model, and using Methods A, B and C. RAOBS data collected at Stornway, UK.

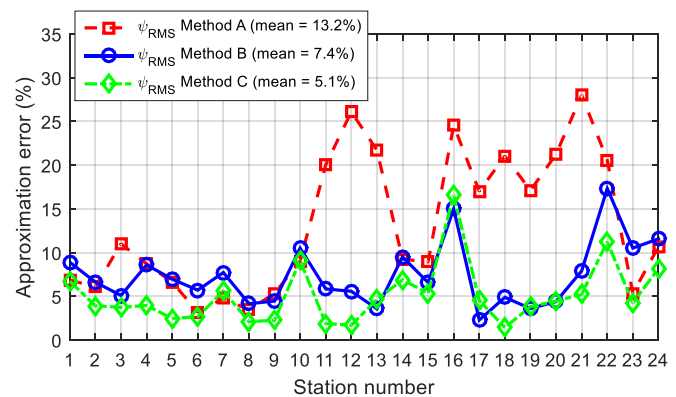


Fig. 3. Mean E ( $\psi_E$ ) and mean RMS ( $\psi_{RMS}$ ) as a function RAOBS site (average over all frequencies from 1 to 350 GHz with 10-GHz step).

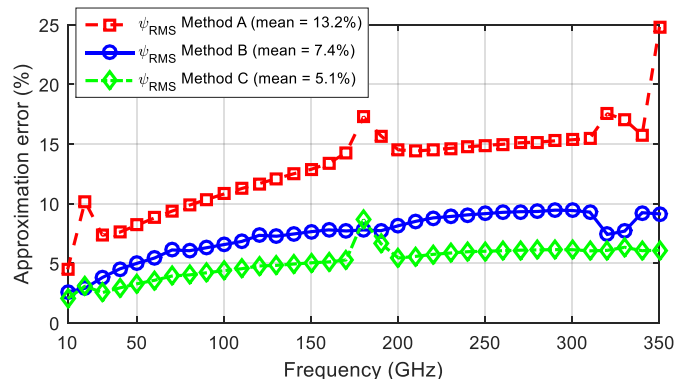


Fig. 4. Mean E ( $\psi_E$ ) and mean RMS ( $\psi_{RMS}$ ) as a function of frequency (average over all stations).

A closer inspection of the results in Fig. 3 indicates that, although for some sites Method A shows a better average performance, it also exhibits a larger spread in the resulting RMS than that associated to the prediction methods receiving as input  $V$ . As already mentioned, this is likely due to the

variability of the water vapor scale height  $V_{SH}$  with latitude, season and climate, which is not reflected in the equations of Method A. In addition, Fig 3 also shows that the modifications to the method in [7] lead to performance improvements across almost all sites. This is confirmed also by the results in Fig. 4: as frequency increases, the prediction error increases for all models, but at a slower rate for Method C.

Based on these results, we conclude that, when local atmospheric profiles are not available, Method C, based on integrated water vapor content data that can be extracted from the digital maps attached to recommendation P.836-5, should be preferred for the prediction of attenuation due to water vapor on slant paths with an elevation angle greater than 5 degrees, in the 1-350 GHz frequency range.

## V. CONCLUSIONS

This contribution introduces an improved method for the prediction of the statistics of  $A_V$  for Earth-space slant paths, with elevation angles greater than 5 degrees, and provides guidance towards the selection of the most suitable model for the prediction of  $A_V$  when local atmospheric profiles are not available.

The analyses carried out in this paper indicate that the improved method described in section III.C, using as input statistics of integrated water vapor content readily available from the ITU-R, should be preferred over the methods currently provided in Annex 2 of recommendation ITU-R P.676-10, using either surface water vapor density data or integrated water vapor statistics. This result is important as it sheds light on the current ambiguity in recommendation P.676-10 as to which approximate model should be selected for predictions along Earth-space slant paths.

## ACKNOWLEDGMENT

The authors would like to acknowledge Dr. Martellucci from the European Space Agency for the provision of FERAS radiosonde data.

## REFERENCES

- [1] A. Paraboni, C. Riva, L. Valbonesi, M. Mauri, "Eight Years of ITALSAT Copolar Attenuation Statistics at Spino d'Adda", *Space Communications*, Vol. 18, No. 1-2, 2002, pp. 59-64.
- [2] H. J. Liebe, G. A. Hufford, and M. G. Cotton, "Propagation modeling of moist air and suspended water/ice particles at frequencies below 1000 GHz," in *Proc. AGARD 52nd Spec. Meeting EM Wave Propag. Panel*, Palma De Maiorca, Spain, 1993, pp. 3.1-3.10.
- [3] P. Rosenkranz, "Water vapor microwave continuum absorption: A comparison of measurements and models," *Radio Sci.*, vol. 33, no. 4, pp. 919-928, Jul./Aug. 1998.
- [4] P. Bouchard, "Approximate Method for Estimating Gaseous Loss at Very Low Angles Along Paths of Finite Length and Earth-Space Paths," *IEEE Transactions on Antennas and Propagation*, vol. 64, no. 2, Page(s): 687 - 699, February 2016.
- [5] Attenuation by atmospheric gases. Geneva, 2013, ITU-R recommendation P.676-10.
- [6] Water vapour: surface density and total columnar content. Geneva, 2013, ITU-R recommendation P.836-5.
- [7] L. Luini, C. Riva, "Improving the Accuracy in Predicting Water Vapor Attenuation at Millimeter-wave for Earth-space Applications," *IEEE Transactions on Antennas and Propagation*, vol. 64, no. 6, Page(s): 2487 - 2493, June 2016.

- [8] L. Luini, C. Riva, C. Capsoni, A. Martellucci, "Attenuation in non rainy conditions at millimeter wavelengths: assessment of a procedure," *IEEE Transactions on Geoscience and Remote Sensing*, pp. 2150-2157, Vol. 45, Issue 7, July 2007.
- [9] COST Action 255 Final Report, "Precipitation, Clouds and Other Related Non-Refractive Effects," J. P. V. Poiars Baptista, Ed. Noordwijk, The Netherlands: ESA Publication Division, ch. 3.2.
- [10] E. Salonen, S. Karhu, P. Jokela, W. Zhang, S. Uppala, H. Aulamo, S. Sarkkula, "Study of propagation phenomena for low availabilities," Helsinki University of Technology Radio Laboratory and Finnish Meteorological Institute, Finland, Final Report for the European Space Agency under ESTEC contract 8025/88/NL/PR, Nov. 1990.
- [11] Acquisition, presentation and analysis of data in studies of tropospheric propagation. Geneva, 2015, ITU-R recommendation P.311-15.